

Lim, Susan^{1,2,3}, Tang, GC Kerrie¹, Lam FL³, Karuppasamy, J¹, Sakban, R¹, Ma FJ², Lee EH¹, Soria, B^{1,4}

¹ Department of Orthopaedic Surgery, National University of Singapore, Singapore

² Stem Cell Technologies (i), Singapore.

³ Susan Lim Surgery, Centre for Breast Screening & Surgery, Singapore **Email: sl@susanlimsurgery.com**

⁴ Centro Andaluz de Biología Molecular y Medicina Regenerativa (CABIMER), Seville, Spain

Cancer-associated fibroblasts/myofibroblasts and inflammatory cells produce a vast array of growth factors, chemokines and extracellular matrix (ECM) components that facilitate cancer progression, invasion/metastasis and neovascularisation. In this work, the aim was to describe the isolation and characterization of human adipose-derived mesenchymal cells from the stroma of both benign and malignant breast tissues and also to identify the differences in the array of growth factors and cytokines from benign and malignant mesenchymal stem cells.

Methods

Excised adipose tissue was finely minced with a scalpel and collagenase-digested to liberate cells from connective tissue. Following centrifugation and filtration, the resulting cell pellet was seeded into cell culture flasks.

Cells were cultured in media comprising DMEM/F-12 containing 10%FCS, 10ng/ml bFGF and 1% pen/strep. Cells were trypsinised with 0.5mM/0.05% trypsin when subconfluent.

Cells counts were performed at each passage and Population Doublings (PD) and Times (PDTs) were calculated using the following formulae:

$$PD = \frac{\log Y - \log X}{0.301} \quad PDT = \frac{T \times \log 2}{\log Y - \log X}$$

Y = cell nos. at end of passage
X = cell nos. seeded at start
T = days in culture

Adipose-derived MSCs (Ad-MSCs) between passages 1 to 6 were used for all experiments. Phenotypic characterisation was performed by flow cytometry with a panel of fluorescently-labelled specific antibodies.

Lineage	Induction Media	Lineage markers
Adipogenic	DMEM/F12, 20ng dHFD, 10ng TGF-β1, 10ng IGF-1, 10ng PDGF-β, 10ng FGF-2, 10ng bFGF, 10ng TGF-α, 10ng TGF-β1, 10ng TGF-β2, 10ng TGF-β3, 10ng TGF-β4, 10ng TGF-β5, 10ng TGF-β6, 10ng TGF-β7, 10ng TGF-β8, 10ng TGF-β9, 10ng TGF-β10, 10ng TGF-β11, 10ng TGF-β12, 10ng TGF-β13, 10ng TGF-β14, 10ng TGF-β15, 10ng TGF-β16, 10ng TGF-β17, 10ng TGF-β18, 10ng TGF-β19, 10ng TGF-β20, 10ng TGF-β21, 10ng TGF-β22, 10ng TGF-β23, 10ng TGF-β24, 10ng TGF-β25, 10ng TGF-β26, 10ng TGF-β27, 10ng TGF-β28, 10ng TGF-β29, 10ng TGF-β30, 10ng TGF-β31, 10ng TGF-β32, 10ng TGF-β33, 10ng TGF-β34, 10ng TGF-β35, 10ng TGF-β36, 10ng TGF-β37, 10ng TGF-β38, 10ng TGF-β39, 10ng TGF-β40, 10ng TGF-β41, 10ng TGF-β42, 10ng TGF-β43, 10ng TGF-β44, 10ng TGF-β45, 10ng TGF-β46, 10ng TGF-β47, 10ng TGF-β48, 10ng TGF-β49, 10ng TGF-β50, 10ng TGF-β51, 10ng TGF-β52, 10ng TGF-β53, 10ng TGF-β54, 10ng TGF-β55, 10ng TGF-β56, 10ng TGF-β57, 10ng TGF-β58, 10ng TGF-β59, 10ng TGF-β60, 10ng TGF-β61, 10ng TGF-β62, 10ng TGF-β63, 10ng TGF-β64, 10ng TGF-β65, 10ng TGF-β66, 10ng TGF-β67, 10ng TGF-β68, 10ng TGF-β69, 10ng TGF-β70, 10ng TGF-β71, 10ng TGF-β72, 10ng TGF-β73, 10ng TGF-β74, 10ng TGF-β75, 10ng TGF-β76, 10ng TGF-β77, 10ng TGF-β78, 10ng TGF-β79, 10ng TGF-β80, 10ng TGF-β81, 10ng TGF-β82, 10ng TGF-β83, 10ng TGF-β84, 10ng TGF-β85, 10ng TGF-β86, 10ng TGF-β87, 10ng TGF-β88, 10ng TGF-β89, 10ng TGF-β90, 10ng TGF-β91, 10ng TGF-β92, 10ng TGF-β93, 10ng TGF-β94, 10ng TGF-β95, 10ng TGF-β96, 10ng TGF-β97, 10ng TGF-β98, 10ng TGF-β99, 10ng TGF-β100	Leptin accumulation (Oil-Red-O), PPAR-γ, CD136, CD137, CD138, CD139, CD140, CD141, CD142, CD143, CD144, CD145, CD146, CD147, CD148, CD149, CD150, CD151, CD152, CD153, CD154, CD155, CD156, CD157, CD158, CD159, CD160, CD161, CD162, CD163, CD164, CD165, CD166, CD167, CD168, CD169, CD170, CD171, CD172, CD173, CD174, CD175, CD176, CD177, CD178, CD179, CD180, CD181, CD182, CD183, CD184, CD185, CD186, CD187, CD188, CD189, CD190, CD191, CD192, CD193, CD194, CD195, CD196, CD197, CD198, CD199, CD200, CD201, CD202, CD203, CD204, CD205, CD206, CD207, CD208, CD209, CD210, CD211, CD212, CD213, CD214, CD215, CD216, CD217, CD218, CD219, CD220, CD221, CD222, CD223, CD224, CD225, CD226, CD227, CD228, CD229, CD230, CD231, CD232, CD233, CD234, CD235, CD236, CD237, CD238, CD239, CD240, CD241, CD242, CD243, CD244, CD245, CD246, CD247, CD248, CD249, CD250, CD251, CD252, CD253, CD254, CD255, CD256, CD257, CD258, CD259, CD260, CD261, CD262, CD263, CD264, CD265, CD266, CD267, CD268, CD269, CD270, CD271, CD272, CD273, CD274, CD275, CD276, CD277, CD278, CD279, CD280, CD281, CD282, CD283, CD284, CD285, CD286, CD287, CD288, CD289, CD290, CD291, CD292, CD293, CD294, CD295, CD296, CD297, CD298, CD299, CD300, CD301, CD302, CD303, CD304, CD305, CD306, CD307, CD308, CD309, CD310, CD311, CD312, CD313, CD314, CD315, CD316, CD317, CD318, CD319, CD320, CD321, CD322, CD323, CD324, CD325, CD326, CD327, CD328, CD329, CD330, CD331, CD332, CD333, CD334, CD335, CD336, CD337, CD338, CD339, CD340, CD341, CD342, CD343, CD344, CD345, CD346, CD347, CD348, CD349, CD350, CD351, CD352, CD353, CD354, CD355, CD356, CD357, CD358, CD359, CD360, CD361, CD362, CD363, CD364, CD365, CD366, CD367, CD368, CD369, CD370, CD371, CD372, CD373, CD374, CD375, CD376, CD377, CD378, CD379, CD380, CD381, CD382, CD383, CD384, CD385, CD386, CD387, CD388, CD389, CD390, CD391, CD392, CD393, CD394, CD395, CD396, CD397, CD398, CD399, CD400, CD401, CD402, CD403, CD404, CD405, CD406, CD407, CD408, CD409, CD410, CD411, CD412, CD413, CD414, CD415, CD416, CD417, CD418, CD419, CD420, CD421, CD422, CD423, CD424, CD425, CD426, CD427, CD428, CD429, CD430, CD431, CD432, CD433, CD434, CD435, CD436, CD437, CD438, CD439, CD440, CD441, CD442, CD443, CD444, CD445, CD446, CD447, CD448, CD449, CD450, CD451, CD452, CD453, CD454, CD455, CD456, CD457, CD458, CD459, CD460, CD461, CD462, CD463, CD464, CD465, CD466, CD467, CD468, CD469, CD470, CD471, CD472, CD473, CD474, CD475, CD476, CD477, CD478, CD479, CD480, CD481, CD482, CD483, CD484, CD485, CD486, CD487, CD488, CD489, CD490, CD491, CD492, CD493, CD494, CD495, CD496, CD497, CD498, CD499, CD500, CD501, CD502, CD503, CD504, CD505, CD506, CD507, CD508, CD509, CD510, CD511, CD512, CD513, CD514, CD515, CD516, CD517, CD518, CD519, CD520, CD521, CD522, CD523, CD524, CD525, CD526, CD527, CD528, CD529, CD530, CD531, CD532, CD533, CD534, CD535, CD536, CD537, CD538, CD539, CD540, CD541, CD542, CD543, CD544, CD545, CD546, CD547, CD548, CD549, CD550, CD551, CD552, CD553, CD554, CD555, CD556, CD557, CD558, CD559, CD560, CD561, CD562, CD563, CD564, CD565, CD566, CD567, CD568, CD569, CD570, CD571, CD572, CD573, CD574, CD575, CD576, CD577, CD578, CD579, CD580, CD581, CD582, CD583, CD584, CD585, CD586, CD587, CD588, CD589, CD590, CD591, CD592, CD593, CD594, CD595, CD596, CD597, CD598, CD599, CD600, CD601, CD602, CD603, CD604, CD605, CD606, CD607, CD608, CD609, CD610, CD611, CD612, CD613, CD614, CD615, CD616, CD617, CD618, CD619, CD620, CD621, CD622, CD623, CD624, CD625, CD626, CD627, CD628, CD629, CD630, CD631, CD632, CD633, CD634, CD635, CD636, CD637, CD638, CD639, CD640, CD641, CD642, CD643, CD644, CD645, CD646, CD647, CD648, CD649, CD650, CD651, CD652, CD653, CD654, CD655, CD656, CD657, CD658, CD659, CD660, CD661, CD662, CD663, CD664, CD665, CD666, CD667, CD668, CD669, CD670, CD671, CD672, CD673, CD674, CD675, CD676, CD677, CD678, CD679, CD680, CD681, CD682, CD683, CD684, CD685, CD686, CD687, CD688, CD689, CD690, CD691, CD692, CD693, CD694, CD695, CD696, CD697, CD698, CD699, CD700, CD701, CD702, CD703, CD704, CD705, CD706, CD707, CD708, CD709, CD710, CD711, CD712, CD713, CD714, CD715, CD716, CD717, CD718, CD719, CD720, CD721, CD722, CD723, CD724, CD725, CD726, CD727, CD728, CD729, CD730, CD731, CD732, CD733, CD734, CD735, CD736, CD737, CD738, CD739, CD740, CD741, CD742, CD743, CD744, CD745, CD746, CD747, CD748, CD749, CD750, CD751, CD752, CD753, CD754, CD755, CD756, CD757, CD758, CD759, CD760, CD761, CD762, CD763, CD764, CD765, CD766, CD767, CD768, CD769, CD770, CD771, CD772, CD773, CD774, CD775, CD776, CD777, CD778, CD779, CD780, CD781, CD782, CD783, CD784, CD785, CD786, CD787, CD788, CD789, CD790, CD791, CD792, CD793, CD794, CD795, CD796, CD797, CD798, CD799, CD800, CD801, CD802, CD803, CD804, CD805, CD806, CD807, CD808, CD809, CD810, CD811, CD812, CD813, CD814, CD815, CD816, CD817, CD818, CD819, CD820, CD821, CD822, CD823, CD824, CD825, CD826, CD827, CD828, CD829, CD830, CD831, CD832, CD833, CD834, CD835, CD836, CD837, CD838, CD839, CD840, CD841, CD842, CD843, CD844, CD845, CD846, CD847, CD848, CD849, CD850, CD851, CD852, CD853, CD854, CD855, CD856, CD857, CD858, CD859, CD860, CD861, CD862, CD863, CD864, CD865, CD866, CD867, CD868, CD869, CD870, CD871, CD872, CD873, CD874, CD875, CD876, CD877, CD878, CD879, CD880, CD881, CD882, CD883, CD884, CD885, CD886, CD887, CD888, CD889, CD890, CD891, CD892, CD893, CD894, CD895, CD896, CD897, CD898, CD899, CD900, CD901, CD902, CD903, CD904, CD905, CD906, CD907, CD908, CD909, CD910, CD911, CD912, CD913, CD914, CD915, CD916, CD917, CD918, CD919, CD920, CD921, CD922, CD923, CD924, CD925, CD926, CD927, CD928, CD929, CD930, CD931, CD932, CD933, CD934, CD935, CD936, CD937, CD938, CD939, CD940, CD941, CD942, CD943, CD944, CD945, CD946, CD947, CD948, CD949, CD950, CD951, CD952, CD953, CD954, CD955, CD956, CD957, CD958, CD959, CD960, CD961, CD962, CD963, CD964, CD965, CD966, CD967, CD968, CD969, CD970, CD971, CD972, CD973, CD974, CD975, CD976, CD977, CD978, CD979, CD980, CD981, CD982, CD983, CD984, CD985, CD986, CD987, CD988, CD989, CD990, CD991, CD992, CD993, CD994, CD995, CD996, CD997, CD998, CD999, CD1000

Table 1

48-hour conditioned culture media were collected from samples and layered onto the cytokine arrays (RayBio® Human Cytokine Antibody Array, C series 1000) and detection performed according to manufacturer's instructions.

Immunocytochemistry: Subconfluent cells were fixed in 4% formaldehyde, followed by a permeabilisation step and stained with mouse anti-ASMA (alpha smooth muscle actin) monoclonal antibody (Dako). Staining was visualised using the UltraVision LPvalue Detection system with AEC substrate (Thermo FisherScientific), according to manufacturer's instructions.

Results and Discussion

Growth and Expansion Characteristics

Ad-MSCs displayed a fibroblast-like morphology (Figure 1A) which was maintained for the entire duration of the culture (4 passages) studied. However, cells tended to exhibit a larger and flatter morphology when progressively passaged (greater than 12 passages) (Figure 1B).

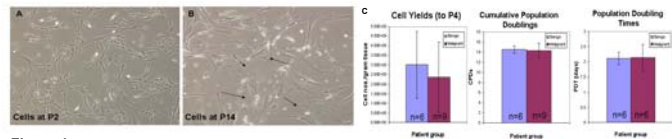


Figure 1 Phase contrast microscopic images of Ad-MSCs at two different stages in culture. A) Ad-MSCs at passage 2 exhibited fibroblast-like morphology. B) Ad-MSCs at passage 14 are larger, with a wide and flat morphology (arrows). All images are at x100mag. C) Growth characteristics of Ad-MSCs. Samples were divided into Benign and Malignant groups. All parameters were calculated for cultures expanded to the fourth passage, in order to avoid potential effects of prolonged culture. Results are expressed as Mean ± Std Dev.

To facilitate comparisons between groups, we computed the expandable cell yields, cumulative population doublings (CPDs) and population doubling times (PDTs) up to the fourth passage. No significant differences between the two patient groups were found for all parameters (Figure 1C), indicating that Ad-MSCs derived from both patient groups exhibited very similar growth characteristics.

Flow cytometric analyses revealed the immunophenotype of Ad-MSCs to be similar for that described for MSCs, i.e. positive for HLA Class I, CD29, CD44, CD73, CD90, CD105 and CD166 (Table 2, Mean > 80%). Reactivities of antibodies against several antigens were significant (Mean ≤ 80%) but showed some degree of variation. These included CD9, CD49d and CD271. In some samples, we also detected small populations of cells expressing the Stro-1 antigen, which has been identified as a multipotential marker in bone-marrow MSCs (Dennis et al, 2002). Ad-MSCs were negative for haematopoietic lineage markers CD14, CD34 and CD45. Interestingly, significant percentages of HLA-DR positive Ad-MSCs were found in our samples, notably samples belonging to the Malignant group. MSCs are not known to express HLA-DR. The significance of this observation warrants further investigation.

Antigen	Benign group, n# (range)	Malignant group, n# (range)
HLA Class I	87.26±3.75% (80.33-97.87%)	87.4±1.25% (80.53-98.97%)
HLA-DR	7.25±1.71% (0-23.3%)	38.8±10.25% (0-49.3%)
CD34	25.8±10.25% (0-35.43-33%)	38.8±10.25% (0-49.3-22%)
CD14	2.0±1.01% (0-3.3%)	1.5±0.41% (0-3.3%)
CD19	19.7±2.01% (10-30.88-88%)	81.8±10.54% (67-93.88-98%)
CD33	0.8%	0.8%
CD34	1.9±0.95% (0-3.3%)	2.0±1.42% (0-4.3%)
CD40	87.8±0.62% (80.79-98.46%)	87.2±0.61% (80.45-98.20%)
CD45	4.7±0.72% (0-1.9%)	1.9±0.42% (0-3.3%)
CD46	94.8±0.28% (77.58-93.83%)	92.5±0.19% (78.19-97.98%)
CD73	90.5±0.49% (87.33-98.89%)	87.2±1.24% (80.53-98.97%)
CD90	80.4±3.12% (60.79-98.19%)	80.5±1.79% (62.33-98.30%)
CD105	83.8±10.53% (51.58-98.49%)	88.9±0.42% (80.79-98.46%)
CD166	8.2±0.77% (0-11.86%)	10.7±0.79% (0-15.31-22%)
CD117	1.7±0.19% (0-3.3%)	1.9±0.88% (0-3.3%)
CD132	0.8%	0.8%
CD166	80.5±1.25% (80.53-83.30%)	88.4±10.87% (80.53-98.97%)
CD271	10.1±0.14% (11.88-83.83%)	37.8±0.32% (0-43.17%)
Stro-1	4.5±1.81% (0-8.47-17%)	7.1±0.41% (0-10.80%)

Table 2 Summary of Ad-MSC immunophenotype as determined by single-colour flow cytometric analysis. The table shows percentage of positive cells for the antigen of interest and are expressed as Mean ± Std Dev.

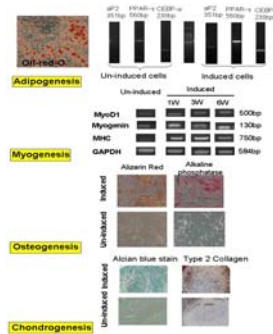


Figure 2 Lineage differentiation of Ad-MSCs. Ad-MSCs were induced to differentiate along 4 lineages in induction media. Differentiation was then confirmed by assessing appropriate markers of differentiation.

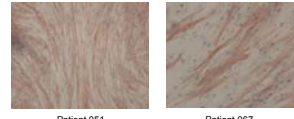


Figure 3 Breast mesenchymal stem cells were stained for the expression of ASMA. Nuclei was counterstained with Harris haematoxylin. Images were taken at x200 mag.

Cultured Ad-MSCs were also positive for the expression of ASMA, although the distribution of expression was heterogeneous (Figure 3). Detection of cytokines by antibody arrays gave a global profile of secreted cytokines in the conditioned media (Figure 4; Table 3). The majority of secreted cytokines identified by array analysis possessed mitogenic, chemotactic, metastatic or pro-angiogenic activities. Hence these cytokines are potentially able to enhance tumour progression, through complex interactions between Ad-MSCs, tumour cells, infiltrating immune cells and other resident cell types in the breast stroma.

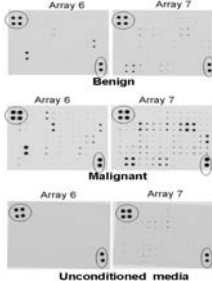


Figure 4 Cytokine array results of conditioned media collected from Ad-MSCs (Benign and Malignant). Representative results from each patient group are shown. Circled spots are array's positive control.

Conditioned Media from Benign Samples		Conditioned Media from Malignant Samples	
ENA-78	GTR	ENA-78	GTR
GRO	GRO-α	GRO	GRO-α
IGFBP-6	IL-8	IGFBP-6	IL-8
TMP-1	TMP-2	TMP-1	TMP-2
UPAR	VEGF	UPAR	VEGF
GCP-2	IL-6	GCP-2	IL-6
MCP-1		MCP-1	
	Angiogenin	Endostatin	
	IGFBP-4	IGFBP-4	
	RANTES	Angiopoietin-2	
	hGF	C-TACK	
	FasTNFRSF-6	FGF-4	
	FGF-9	GTR-ig	
	IL-12p40	IL-12p70	
	IL-25α	IL-6R	
	h-TAC	Lymphotactin	
	MIP-1	MIP-1α	
	MIP-1β	MSP-α	
	Osteopontin	Oncofostin M	
	PGF	Spr150	
	hTNF RII	hTNF RI	
	Thrombospondin	TRAIL-3	
	TRAIL-4		

Table 3 List of cytokines detected in conditioned media from Ad-MSCs (Benign & Malignant). Cytokines in bold type are found in both sample groups, whilst those in normal type are found only in the Malignant group. Cytokines in bold type (except for IL-6) were significantly up-regulated in Malignant samples (p ≤ 0.05).

Summary

We have isolated and characterised Ad-MSCs from breast tissue specimens. Ad-MSCs were easily propagated and culture-expanded. Under the current study criteria, no significant differences in growth characteristics were noted for samples derived from either patient group. Breast Ad-MSCs expressed HLA Class I, CD29, CD44, CD73, CD90, CD105 and CD166 whilst they were negative for CD14, CD34 and C45. However, HLA-DR expression was detected in the majority of samples isolated from donors diagnosed with breast malignancies. We have also shown the multipotent attribute of Ad-MSCs by demonstrating their ability to undergo *in vitro* differentiation, along the adipogenic, chondrogenic, osteogenic and myogenic lineages. Differences in the cytokine profiles secreted by Ad-MSCs from benign and malignant group were noted. There was a significant upregulation of an array of cytokines in the malignant samples as shown in Table 3. The further investigation of this observation may help in the understanding of the roles of cytokines in cancer progression and in identifying potential targets for effective therapy.

Reference:

Dennis JE, Carillet JP, Caplan AL and Charbord P. (2002) Cells Tissues Organs, 170:p73-82.

We gratefully acknowledge the Lee Foundation, Singapore and the Administrative staff of Susan Lim Surgery.